Verification of Deformation Measurement Method Based on FBG Sensor

Zhen Ma[1,2], Xiyuan Chen[1,2](✉), and Junwei Wang[1,2]

[1] The School of Instrument Science and Engineering, Southeast University, Nanjing 210096, China
chxiyuan@seu.edu.cn

[2] Key Laboratory of Micro-Inertial Instrument and Advanced Navigation Technology of Ministry of Education, Southeast University, Nanjing 210096, China

Abstract. Fiber Bragg grating (FBG) sensors are widely used because of their advantages of light weight, corrosion resistance, electromagnetic interference resistance and long life, especially in the field of aerospace. In order to meet the requirements of deformation measurement and structural evaluation of the new generation aircraft, and improve the performance and safety of aircraft, it is of great significance to carry out the research on condition monitoring technology based on FBG sensor in dynamic flight state. In the paper, FBG sensors are applied to the measurement of aircraft wing and the results show that the measurement accuracy of FBG sensor can reach at 1 mm, which has good performance.

Keywords: FBG · Aircraft wing · Measurement

1 Introduction

In recent years, optical fiber measurement technology has been widely used in bridge, dam, tunnel and other large structures [1, 2]. The application of optical fiber measurement technology in the field of aircraft measurement began to be studied in the early 21st century [3–5]. The results show that FBG sensor is very suitable for aircraft strain measurement. On the one hand, FBG sensor has the advantages of small size and light weight. The aircraft structure strain measurement which needs a large number of sensors, the cost of FBG sensor is very cheap. On the other hand, FBG sensor is non-conductive and anti electromagnetic interference, which can be used in noise, corrosion or high-pressure environment. At the same time, due to the multiplicity of optical sensor, FBG sensor can monitor high-density strain distribution in a long distance with only one fiber.

2 Construction of Experimental Platform

FBG sensor can write multiple gratings in one fiber to form a sensing array. As a unique technology of fiber sensor, sensor multiplexing can realize the measurement of distributed field along the fiber laying path. According to the shape and structure characteristics of the real aircraft wing, considering the irregularity of the wing beam section

W. Fu et al. (Eds.): ICMTEL 2021, LNICST 387, pp. 437–441, 2021.
https://doi.org/10.1007/978-3-030-82562-1_41

structure, the two sides of the simulated wing are connected by splicing and fixed on the motion simulation platform with the upper pressure plate. The upper surfaces of both wings are designed to be streamline, which accords with the real wing modal characteristics. The single wing length is 3000 mm, the airfoil length is 2700 mm, the root chord length is 320mm, and the wingtip chord length is 240 mm. Then, the FBG sensor is pasted on the wing surface. The wing structure and FBG sensor installation diagram are shown in Fig. 1. 14 nodes are selected as measurement points on each FBG sensor. The Bragg wavelength of each point is different, and the wavelength range is from 1529 nm to 1584 nm.

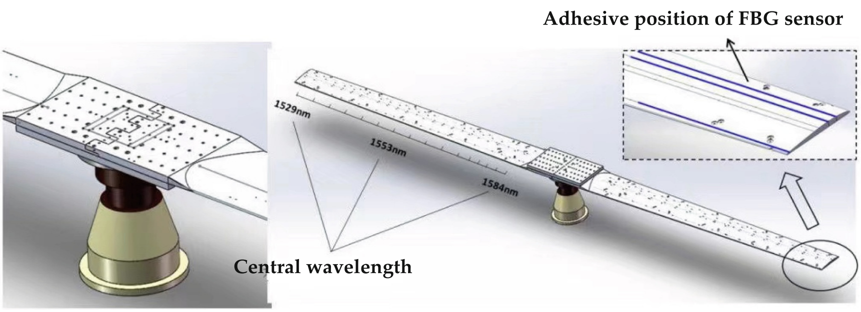

Fig. 1. Wing structure diagram

3 Data Analysis

Due to the asymmetric cross-section of the wing structure, the closer to the root of the wing, the greater the shear force, bending moment and torque on the cross-section are. In the experimental design, the density of FBG sensors is increased at the root of the wing, and four FBG sensor arrays are laid at the root with a spacing of 10 cm. The remaining ten FBG sensor nodes are laid at the far end with a spacing of 20 cm. Two FBGs are installed on the thickest part of the upper and lower surface of the wing. The experimental arrangement is shown in Table 1. The loading method is adopted in the experiment process. The load is continuously applied to one end of the wing to 3 kg. The experimental platform is built as shown in Fig. 2.

Table 1. Measurement experiment scheme

Serial number	Load (kg)	Schedule (s)
1	0	120
2	3	120

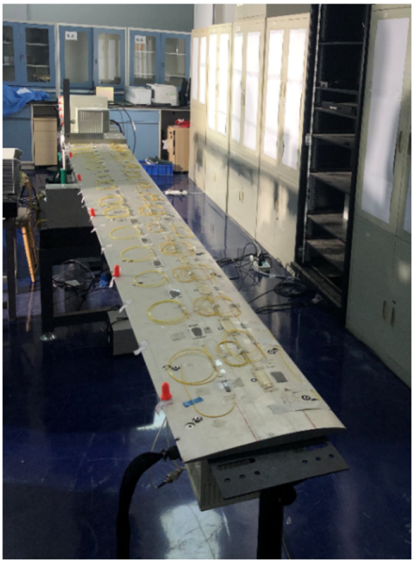

Fig. 2. Physical picture of experimental platform

The data acquisition and processing flow of the wing deformation measurement system based on distributed FBG sensor is as follows:

The FBG demodulator is used to collect the wavelength change data of each point on the upper and lower surface, and make difference with the original wavelength of the corresponding point. At the same time, the strain value of the upper and lower surface is obtained by combining the formula, and the difference value of the strain Center of the upper and lower surface is taken as the strain value under the corresponding load.

The strain change data obtained in step (1) is used to fit the relationship between strain and time, as shown in Fig. 3. It can be seen from the figure that as the pressure

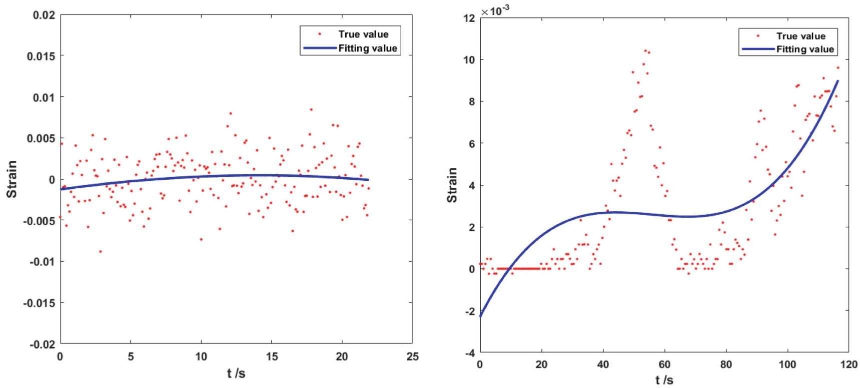

(a) No load applied (b) Apply 3kg load

Fig. 3. Strain fitting results

increases, the strain is gradually increased, and the closer to the root, the greater the strain.

Combined with the height change data of each point of the wing measured by micrometer, the change data and height change data are fitted to obtain the relationship between wing shape variable and position, as shown in Fig. 4.

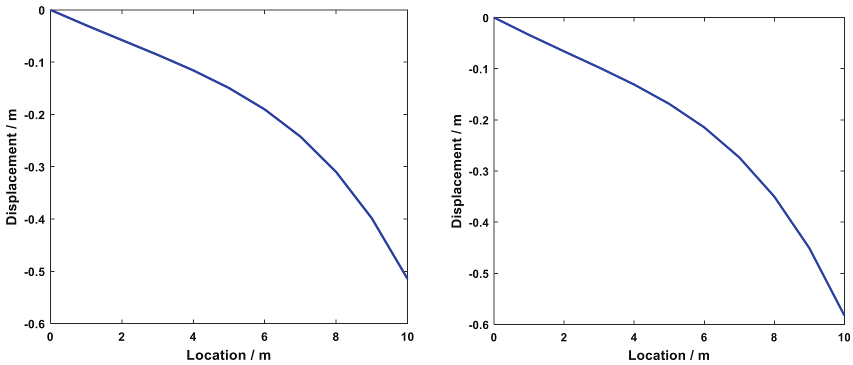

（a）No load applied （b）Apply 3kg load

Fig. 4. Displacement fitting results

By using the fitting model to calculate the shape of the wing at each time, the paper used finite element analysis to verify the accuracy of the deformation displacement model of the wing measured by FBG sensor. According to the deformation displacement results obtained by FBG sensor measurement and fitting, combined with the deformation displacement of finite element analysis in this section, the fitting error of wing end deformation is shown in Table 2. From the table, it can be seen that the error between the fitting value of deformation model based on FBG sensor and the result of finite element analysis is less than 1mm.

Table 2. Fitting error of wing tip deformation

Load (kg)	Fitting value (mm)	Analysis value (mm)	Difference (mm)
0	77.3845	77.0360	0.3485
3	88.2186	87.6760	0.5426

4 Conclusion

Aiming at the problem of flexible multi baseline deformation measurement modeling, the paper analyzes the influence of aircraft wing mechanical structure and aircraft structure force transfer on flexible baseline structure. Based on structural mechanics, the deformation motion law of flexible baseline under interference environment is obtained, and a high-precision deformation modeling method of flexible multi baseline is proposed. Combined with the finite element analysis method, the feasibility and measurement accuracy of the method are verified by experiments, and the maximum error is less than 1 mm.

Acknowledgements. This work was supported by the National Natural Science Foundation of China (No. 61873064 and No. 51375087) and the Scientific Research Foundation of Graduate School of Southeast University (No. YBPY1982).

References

1. Lau, K., Yuan, L., Zhou, L.: Strain monitoring in FRP laminates and concrete beams using FBG sensors. Compos. Struct. **51**, 9–20 (2001)
2. Ma, Z., Chen, X.: Fiber Bragg gratings sensors for aircraft wing shape measurement: recent applications and technical analysis. Sensors **19**(1), 55 (2018). https://doi.org/10.3390/s19010055
3. Wang, J., Chen, X., Yang, P.: Adaptive H-infinite Kalman filter based on multiple fading factors and its application in unmanned underwater vehicle. ISA Trans. (2020). https://doi.org/10.1016/j.isatra.2020.08.030
4. Wang, J., Ma, Z., Chen, X.: Generalized dynamic fuzzy NN model based on multiple fading factors SCKF and its application in integrated navigation. IEEE Sens. J. (2020). https://doi.org/10.1109/JSEN.2020.3022934
5. Yuan, X., Shmaliy, Y.S., Chen, X., Li, Y., Ma, W.: Robust inertial navigation system/ultra wide band integrated indoor quadrotor localization employing adaptive interacting multiple model-unbiased finite impulse response/Kalman filter estimator. Aerosp. Sci. Technol. **98**, 105683 (2020). https://doi.org/10.1016/j.ast.2020.105683